Mem. Fac. Sci. Shimane Univ.,
24, pp. 89–112 Dec. 20, 1990

Ore Minerals of Iwami Kuroko Deposit, Shimane Prefecture, Japan

Takahiro MAKI and Masahide AKASAKA

Department of Geology, Faculty of Science,
Shimane University, 690 Matsue, Japan
(Received September 5, 1990)

Ore minerals of the Iwami kuroko deposits, Shimane Prefecture, have been investigated. The deposits are composed of network and disseminated type deposits, bedded deposits and gypsum deposits. Ore samples collected from the dump are highly silicified and fractured, and are regarded to have derived from the network and disseminated type deposits.

In addition to sphalerite, galena, pyrite, chalcopyrite, tetrahedrite, luzonite and bornite, which were reported so far, tennantite, enargite, covellite, electrum, sylvanite, petzite and hessite have been confirmed. EPMA analyses of ore minerals revealed that the minerals, not only tetrahedrite, tennantite and sphalerite but also others, are more or less variable in composition.

Mineralization sequence in the network and disseminated deposits may be speculated as follows; quartz with fine grained pyrite→sphalerite and galena with small amounts of chalcopyrite, tetrahedrite, electrum and Au-Ag-Te minerals→pyrite and chalcopyrite with small amounts of bornite, covellite, tennantite, luzonite and calcite→luzonite, covellite, calcite and siderite.

Introduction

The Iwami mine is situated in Isotake, Oda City, Shimane Prefecture (Fig. 1). The deposits are composed of kuroko type ores and associated with gypsum deposits. 450000 tons of kuroko ores with 0.8–0.9% Cu, 1.0–1.2% Pb and 6.8–7.5% Zn were produced during the period 1957–1984. At present, the Iwami mine is operated not for kuroko and gypsum ores but for zeolite (IKEDA, 1985).

The Iwami kuroko deposits have been investigated mainly in terms of geology, whereas mineralogical study of kuroko ores has been rare. Although MUKAIYAMA et al. (1974) studied petrography, alteration and fluid inclusions of ores, chemical compositions of most of minerals were not reported.

In the present paper, we report the occurrence, mineral paragenesis and chemical compositions of ore minerals. The mineralization sequence and conditions are also discussed.

Outline of geology and ore deposits

Several works on geology of the Iwami mining area and ore deposits are well summarized in MUKAIYAMA et al. (1974).

The Iwami mining area is geologically composed of Neogene Tertiary and Quaternary strata. The Neogene sediments are divided into the Hata, Kawai, Kuri and Omori Formations in ascending order. Ore deposits of kuroko type are intercalated in the Kuri formation (Fig. 1).

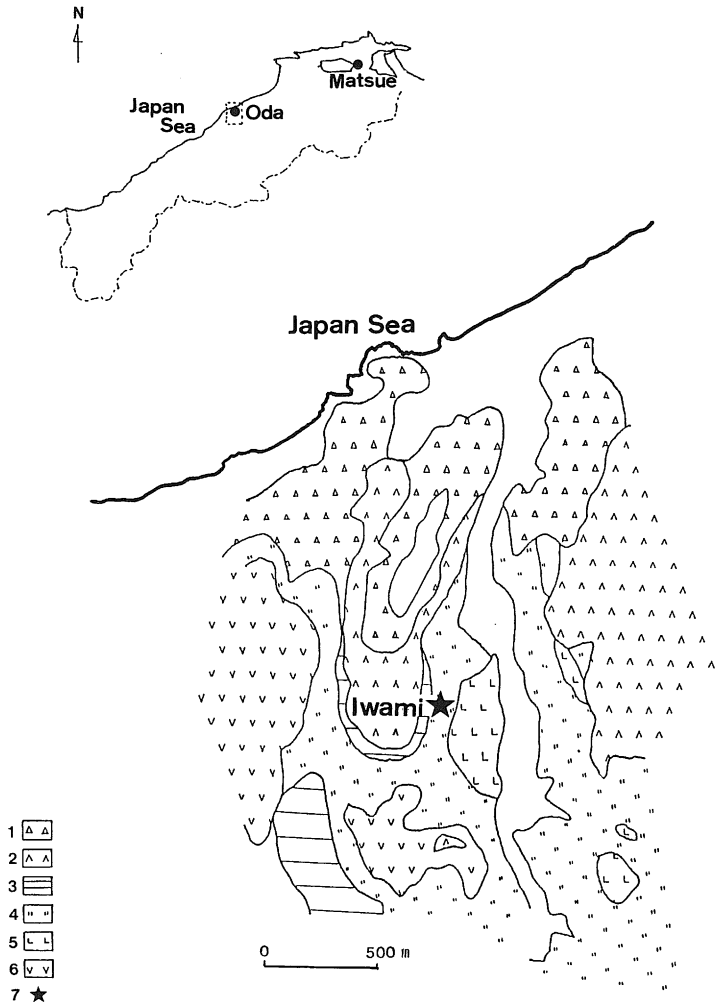

Fig. 1. Geological map and locality of the Iwami deposits (after MITI, 1967).
1: Dolerite of the Omori Formation, 2: Andesite, 3: Upper shale of the Kuri Formation, 4: Breccia, 5: Rhyolite, 6: Yoneyama dacite, 7: Ore deposit.

The Kuri Formation is developed mainly in the Oda basin. Black mudstone is dominated both at the base and top, and dacite, rhyolite and pyroclastics are rich in the intermediate portion. Dacite forms several stratovolcanoes of few hundred meters to three kilometers in diameter. Rhyolite usually forms small intrusive bodies or domes.

The ore deposits of the kuroko type in this district are divided into three types; network and disseminated deposits, gypsum deposits and bedded deposits. Network and disseminated deposits are composed of numerous fractures which are filled with sulfides, and are distributed in altered breccia and rhyolite in the breccia pipe. The deposits and host rocks are silicified. Gypsum deposits consist mainly of alabaster. Bedded deposits are composed of fragments of altered volcanic rocks and ashes, fragments of network ores, fine-grained sulfides and clayey materials.

The network and disseminated deposits of the Iwami mine occur in a breccia pipe of 300 m in diameter at the eastern margin of the Yoneyama dacite body with 3 km in diameter and about 300 m in thickness (Fig. 2). Bedded deposits overlie unconformably network deposits and gypsum deposits. Gypsum deposits occur between network deposits and bedded deposits.

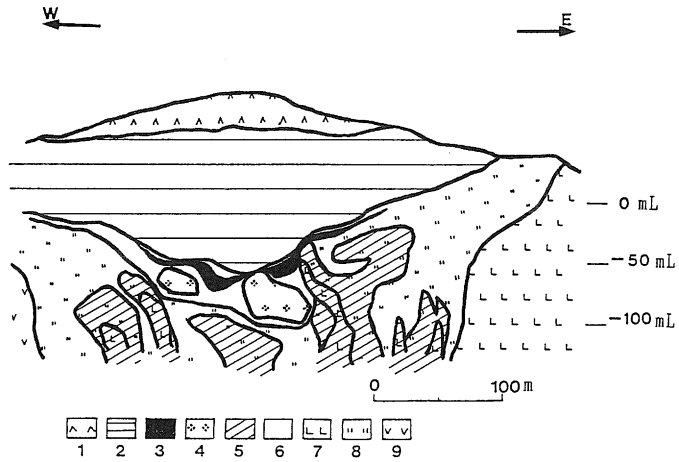

Fig. 2. Cross section (E-W) of one of the ore bodies in the Iwami deposits (after MUKAIYAMA et al., 1974).
1: Andesite of the Omori Formation, 2: Upper shale of the Kuri Formation, 3: Bedded kuroko deposit, 4: Gypsum doposit, 5: Network deposit, 6: Clay bed and argilized rock, 7: Rhyolite, 8: Breccia, 9: Yoneyama dacite.

Occurrence of ore samples

As the old mine openings are closed, ore samples in the present study are collected from the dump. All of the samples are highly silicified and fractured. Thus these ores are regarded to have derived from the network and disseminated deposits. Constituent minerals in ore samples are listed in Table 1.

Table 1. Mineral assemblage of the Iwami deposits

Mineral/Sanple No.	K4	K12	K13	K19	K22	K1	K10	K16	K17	K20	K40	K14	K24
Quartz	◎	◎	◎	◎	◎	◎	◎	◎	◎	○	○	○	◎
Pyrie	·	·	·		·	○	○	◎	◎	○	○	○	○
Sphalerite	·	·		○		○	○	○	○	○	○	○	◎
Galena						○	○	○	○	○	○	◎	
Chalcopyrite	·	·				○	·	○	○	○	○	○	○
Tetrahedrite						·	·	·	·	·	·	·	·
Luzonite						·	·	·	·	·	·		·
Enargite													·
Bornite						·	·	·	·	·		·	·
Covellite						·	·	·	·	·	·	·	·
Electrum						·				·			
Au-Ag-Te mineral										·			
Chlorite					○	○	·			·			
Illite	○		·			○	·	·		·			
Carbonate						·				○	○		

◎ abundant, ○ common, ○ not so common, · rare,

In samples, K2, 3, 7, 8, 11, 15 and 18, omitted in Table 1, quartz is the most dominant mineral, and moderate amount of chlorite and illite are associated. Whereas sulfide minerals are very small in amount and occur only in quartz veinlet.

Samples K14 and K24 are high-grade ores. Sample K14 is mainly composed of galena. The fractures of ore are filled with quartz, galena, pyrite, sphalerite, chalcopyrite, very small amounts of tetrahedrite, bornite and covellite. Sample K24 is composed mainly of brecciated sphalerite grains, less than 1 cm in diameter, and fractures are filled with quartz. Euhedral or unhedral pyrite and chalcopyrite occur in sphalerite and quartz, associated with tennantite and luzonite forming very small grains (Fig. 3).

Other samples are low-grade siliceous ores. In samples K4, 12, 13, 19 and 22, very fine grained pyrite, sphalerite and chalcopyrite distribute in quartz. There are many cavities which are filled with euhedral quartz, pyrite and clay minerals. In samples K1 and 10, small amounts of sphalerite, galena, pyrite and chalcopyrite occur along the fractures. Sphalerite is brecciated and associated with very small amounts of tetrahedrite, luzonite, bornite and covellite (Fig. 4). In samples K16 and 17, pyrite of later stage forms overgrowth on brecciated sphalerite and subhedral pyrite (Fig. 5). In samples 20 and 40, coarse grained sphalerite, galena, chalcopyrite and euhedral pyrite form aggregate in quartz, associated with luzonite, calcite and siderite (Fig. 6).

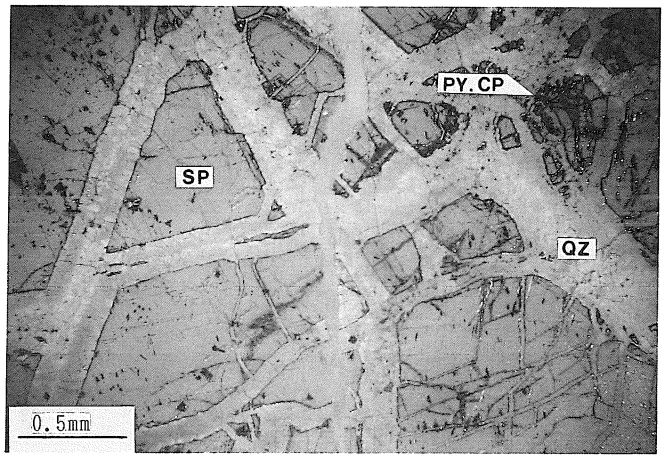

Fig. 3. Photomicrograph of brecciated sphalerite (Sample: K24).
SP: Sphalerite, PY: pyrite, CP: chalocopyrite, QZ: quartz.

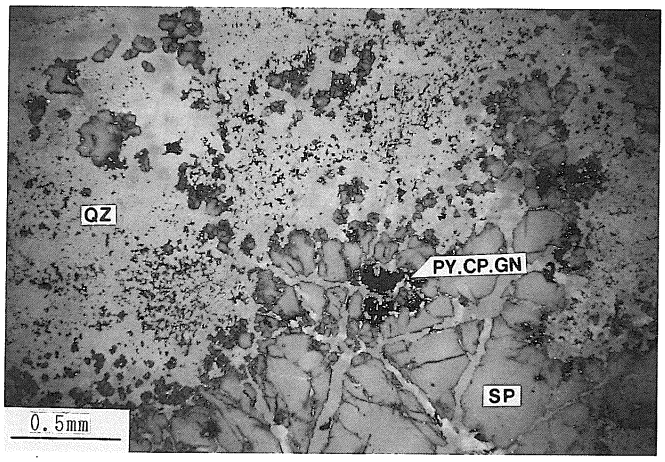

Fig. 4. Photomicrograph of brecciated sphalerite (SP) with pyrite (PY), chalcopyrite (CP) and galena (GN) in the low-grade ore (Sample: K1).

Mineralogy

Analytical method

To make thin sections for microscopic observation and electron microprobe analysis, ore samples were penetrated by regin in vacuum jar and hardened at 60°C for 24 hours, since the ores are generally vesicular and fragile.

Minerals are identified by using ore microscope, X-ray powder diffractometer and electron microprobe analyzer (EPMA). Fine grained carbonates were examined not only by EPMA but also by acid corrosion.

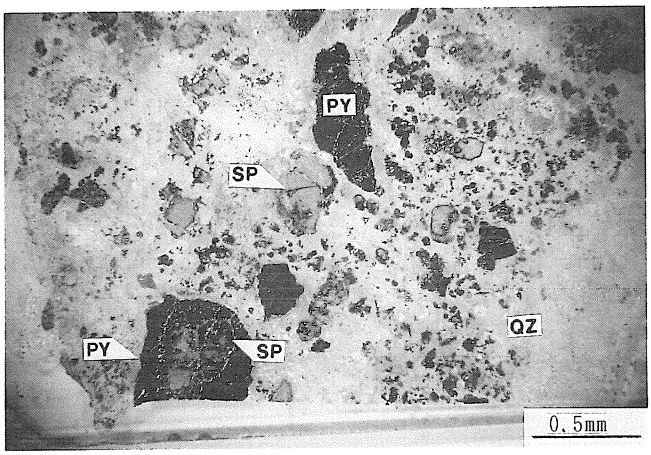

Fig. 5. Photomicrograph of brecciated sphalerite (SP) and overgrowing pyrite (PY) (Sample: K16).

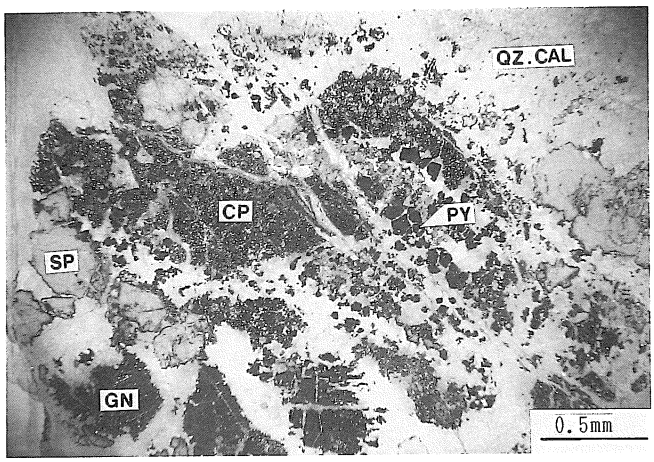

Fig. 6. Photomicrograph of coarse grained sphalerite (SP), galena (GN), chalcopyrite (CP) and pyrite (PY) in quartz (QZ) and calcite (+siderite) (CAL) (Sample: K20).

Chemical analysis was carried out with JEOL JXA-733 electron microprobe. Accelerating voltage, beam current and beam diameter are 20 kV, 0.02 μA and 2–5 μm, respectively. Standards used are synthetic CdS (for Cd, S), Sb_2S_3 (Sb, S), PbS (Pb), Bi_5Se_4S (Bi, Se), MnO (Mn), CoO (Co), NiO (Ni), GaAs (As), metal In, Sn, Bi, Cu, Au, Ag, Te, natural Ag_2S (Ag), ZnS (Zn, S) and Fe_2O_3 (Fe). ZAF correction was employed.

The X-ray powder diffraction was carried out with a RIGAKU X-ray powder diffractometer by using Cu radiation.

Pyrite

Pyrite is common mineral in the ores, and is divided into early stage one and later stage one. Early stage pyrite is euhedral to subhedral form with 0.1 mm in diameter, and distributes in quartz and rim of sphalerite grain. It contains droplike chalcopyrite, bornite, galena and covellite, about 0.01 mm in diameter (Fig. 7). Unhedral pyrite of later stage encloses early stage pyrite (Fig. 8).

Representative analyses are listed in Table 2. Trace amounts of Co, Cu, Zn, Au, Ag, Pb, Bi and As are detected. The compositional difference between early stage pyrite and later stage one is not observed. Rarely greenish yellow region, which is 0.04

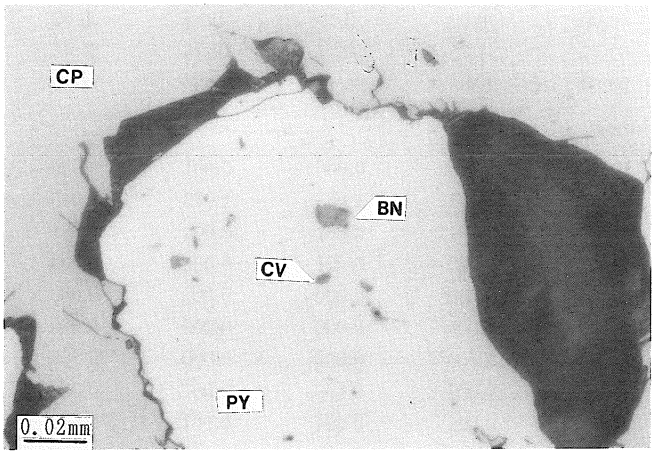

Fig. 7. Photomicrograph showing bornite (BN) and covellite (CV) in pyrite (PY). CP: chalcopyrite

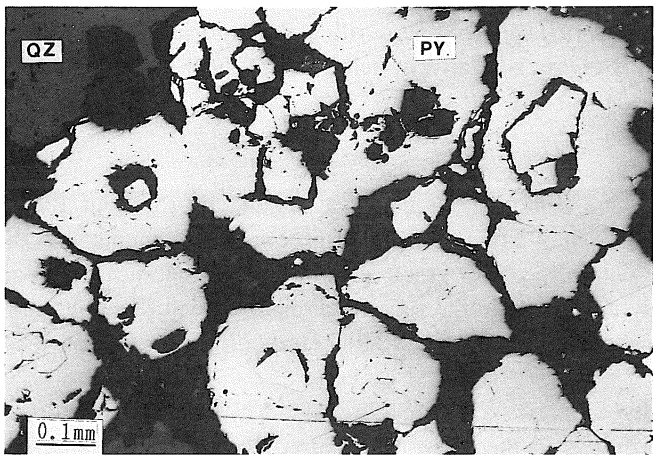

Fig. 8. Photomicrograph showing early stage pyrite (PY) and later stage one.

Table 2. EPMA analyses of pyrite

	K10-103	K14-101	K16-101	K16-105	K20-103	K24-102
Mn	0.00	0.07	0.00	0.06	0.00	0.00
Fe	45.62	47.48	46.75	46.52	46.76	46.36
Co	0.01	0.04	0.00	0.04	0.04	0.01
Cu	0.39	0.00	0.04	1.79	0.01	0.24
Zn	0.00	0.00	0.00	0.00	0.01	0.03
Au	0.00	0.04	0.01	0.00	0.07	0.00
Ag	0.00	0.00	0.00	0.01	0.00	0.00
Pb	0.22	0.31	0.00	0.27	0.20	0.18
Bi	0.17	0.23	0.16	0.23	0.30	0.20
As	0.00	0.02	0.19	0.85	0.02	0.00
S	53.19	51.75	50.97	49.76	51.45	53.24
Total	99.60	99.94	98.12	99.53	98.86	100.26
Structural formula						
Mn	0.000	0.000	0.000	0.001	0.000	0.000
Fe	0.985	1.053	1.053	1.073	1.043	1.000
Co	0.000	0.001	0.001	0.001	0.001	0.000
Cu	0.007	0.000	0.001	0.036	0.000	0.005
Zn	0.000	0.000	0.000	0.000	0.000	0.001
Au	0.000	0.000	0.000	0.000	0.000	0.000
Ag	0.000	0.000	0.000	0.000	0.000	0.000
Pb	0.001	0.002	0.000	0.002	0.001	0.001
Bi	0.001	0.001	0.001	0.001	0.002	0.001
As	0.000	0.000	0.003	0.015	0.000	0.000
S	2.000	2.000	2.000	2.000	2.000	2.000
Total	2.994	3.057	3.059	3.129	3.047	3.008

mm in diameter and rich in very fine cavities, is found in pyrite grain. The chemical composition of this region is relatively rich in Cu (1.79wt.%) and As (0.85 wt.%) (No. K16-105 in Table 2).

Sphalerite

Sphalerite occurs commonly as euhedral crystals up to about 10 mm in diameter, subhedral grains less than 5 mm in size and brecciated fragments with 0.3 to 20 mm in diameter. It is generally yellow green in color, and sometimes shows zonal structure. It shows chalcopyrite disease in the rim and along the fracture and grain boundary (Fig. 9). Sphalerite associated with galena and tetrahedrite has reddish brown band (Fig. 10).

Representative analyses are listed in Table 3. These are almost consistent with sphalerite compositions in the network deposits reported by MUKAIYAMA et al. (1974) and URABE (1974a); Zn 61–68, Fe 0.1–3, Mn 0–0.1, Cu 0–0.6, Cd 0–0.9, Pb 0.05–0.69

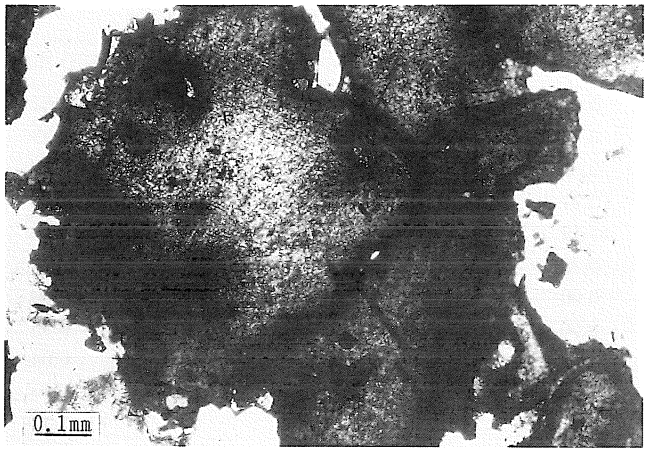

Fig. 9. Photomicrograph showing chalcopyrite disease in sphalerite.

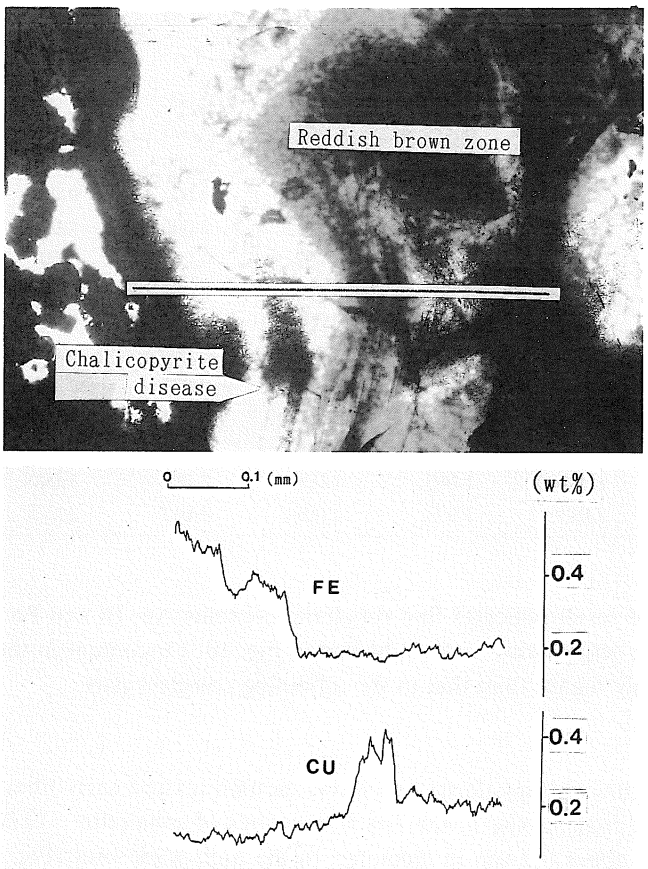

Fig. 10. Reddish brown band in sphalerite and line scan profile for Cu Kα and Fe Kα.

Table 3. EPMA analyses of sphalerite

	K10-204	K14-201	K16-203	K16-204	K20-201	K24-202
Mn	0.03	0.07	0.02	0.01	0.02	0.04
Fe	0.60	0.28	0.44	0.16	0.37	0.97
Co	0.00	0.00	0.00	0.01	0.00	0.01
Cu	0.27	0.09	0.00	0.04	0.24	0.00
Zn	65.19	65.50	65.87	66.30	66.26	66.54
Au	0.38	0.26	0.43	0.39	0.28	0.22
Ag	0.00	0.00	0.00	0.00	0.00	0.04
Cd	0.30	0.24	0.26	0.25	0.35	0.28
In	0.00	0.00	0.00	0.00	0.04	0.02
Pb	0.22	0.19	0.16	0.17	0.13	0.14
Bi	0.20	0.19	0.15	0.15	0.14	0.21
As	0.00	0.04	0.00	0.06	0.00	0.00
S	32.32	32.74	32.70	32.31	32.25	31.92
Total	99.51	99.60	100.03	99.85	100.08	100.39
Structural formula						
Mn	0.000	0.001	0.000	0.000	0.000	0.001
Fe	0.011	0.005	0.008	0.003	0.007	0.017
Co	0.000	0.000	0.000	0.000	0.000	0.000
Cu	0.004	0.001	0.000	0.001	0.004	0.000
Zn	0.989	0.981	0.988	1.006	1.008	1.022
Au	0.002	0.001	0.002	0.002	0.001	0.001
Ag	0.000	0.000	0.000	0.000	0.000	0.000
Cd	0.003	0.002	0.002	0.002	0.003	0.003
In	0.000	0.000	0.000	0.000	0.000	0.000
Pb	0.001	0.001	0.001	0.001	0.001	0.001
Bi	0.001	0.001	0.001	0.001	0.001	0.001
As	0.000	0.000	0.000	0.001	0.000	0.000
S	1.000	1.000	1.000	1.000	1.000	1.000
Total	2.011	1.993	2.002	2.017	2.025	2.046

wt.%. Present result indicates that sphalerite contains Au, Bi and Pb up to 0.43, 0.21 and 0.22 wt.%, respectively. As indicated in Fig. 10, Cu content in the reddish brown band is relatively higher than that in the adjoining colorless part.

Galena

Galena occurs with sphalerite and shows mottled texture each other. It also occurs with pyrite and chalcopyrite in the rim and cavities of sphalerite. Galena often shows euhedral form, about 0.2 mm in diameter, in the high-grade ores (Fig. 11), though it is generally unhedral form, less than 0.2 mm in diameter.

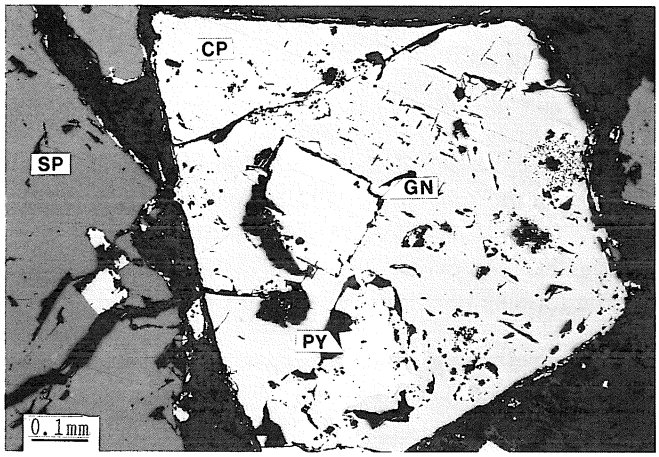

Fig. 11. Euhedral galena (GN) and unhedral pyrite (PY) in chalcopyrite (CP).

Table 4. EPMA analyses of galena

	K10-302	K14-302	K16-301	K20-301
Fe	0.00	0.02	0.01	0.01
Co	0.00	0.01	0.00	0.00
Ni	0.00	0.00	0.00	0.01
Cu	0.01	0.05	0.03	0.00
Zn	0.00	0.00	0.02	0.00
Au	0.00	0.00	0.01	0.03
Cd	0.00	0.03	0.00	0.03
Pb	85.04	87.54	85.77	86.15
Bi	0.44	0.54	0.51	0.41
S	13.40	12.32	13.40	13.44
Total	98.89	100.51	99.75	100.08
Structural formula				
Fe	0.000	0.001	0.000	0.000
Co	0.000	0.000	0.000	0.000
Ni	0.000	0.000	0.000	0.000
Cu	0.001	0.002	0.001	0.000
Zn	0.000	0.000	0.001	0.000
Au	0.000	0.000	0.000	0.000
Cd	0.000	0.001	0.000	0.001
Pb	0.983	1.099	0.991	0.992
Bi	0.005	0.007	0.006	0.005
S	1.000	1.000	1.000	1.000
Total	1.989	2.110	1.999	1.998

Representative analyses of galena are listed in Table 4. It is noted that galena contains 0.41–0.54 wt.% of Bi.

Chalcopyrite

Chalcopyrite encloses the euhedral to subhedral pyrite and euhedral galena (Fig. 11), and fills fractures in the sphalerite. Chalcopyrite and galena often show mottled texture each other. Fine-grained dots of chalcopyrite, about 0.01 mm in diameter, occur in sphalerite, galena and pyrite.

The chalcopyrite forming dots in pyrite contains Ag up to 1.49 wt.% (No. K16-402 in Table 5).

Table 5. EPMA analyses of chalcopyrite

	K1-401	K14-401	K16-402	K20-401
Mn	0.00	0.00	0.03	0.00
Fe	30.81	30.19	30.68	30.48
Co	0.06	0.02	0.05	0.02
Ni	0.05	0.00	0.04	0.00
Cu	33.52	33.48	32.88	33.32
Zn	0.59	0.04	0.14	0.04
Au	0.25	0.06	0.16	0.07
Ag	0.06	0.03	1.49	0.00
Cd	0.02	0.00	0.06	0.00
Pb	0.23	0.15	0.00	0.18
Bi	0.30	0.24	0.15	0.20
As	0.00	0.01	0.14	0.03
S	34.02	34.98	33.93	35.30
Total	99.91	99.20	99.75	99.64
Structural formula				
Mn	0.000	0.000	0.001	0.000
Fe	1.040	0.991	1.038	0.991
Co	0.002	0.001	0.002	0.001
Ni	0.002	0.000	0.001	0.000
Cu	0.994	0.965	0.978	0.952
Zn	0.017	0.001	0.004	0.001
Au	0.002	0.001	0.001	0.001
Ag	0.001	0.001	0.026	0.000
Cd	0.000	0.000	0.001	0.000
Pb	0.002	0.001	0.000	0.002
Bi	0.003	0.002	0.001	0.002
As	0.000	0.000	0.004	0.001
S	2.000	2.000	2.000	2.000
Total	4.063	3.963	4.057	3.951

Tetrahedrite and tennantite

Tetrahedrite occurs as unhedral grain, less than 0.05 mm in diameter, in galena and in the reddish brown band of sphalerite. It also occurs as dots in galena. Tennantite

Table 6. EPMA analyses of tetrahedrite-tennantite

	K1-504	K10-501	K14-501	K14-506	K14-507	K16-506	K16-510	K16-518	K20-502	K24-501
Mn	0.00	0.02	0.00	0.02	0.00	0.00	0.00	0.00	0.01	0.00
Fe	4.09	3.61	2.19	0.59	0.68	1.88	0.62	0.68	0.99	6.91
Co	0.00	0.01	0.01	0.00	0.00	0.00	0.02	0.00	0.00	0.03
Ni	0.00	0.02	0.00	0.00	0.00	0.00	0.00	0.00	0.00	0.01
Cu	42.90	42.44	34.66	35.35	36.93	41.55	37.59	41.82	34.78	43.94
Zn	5.60	4.83	5.13	6.90	5.87	6.98	7.54	8.41	5.75	0.10
Au	0.00	0.20	0.01	0.04	0.09	0.00	0.00	0.00	0.19	0.15
Ag	0.12	0.13	4.18	3.26	1.67	0.04	0.83	0.13	2.84	0.15
Cd	0.00	0.06	0.02	0.05	0.03	0.02	0.04	0.00	0.33	0.02
In	0.00	0.03	0.00	0.00	0.00	0.00	0.00	0.00	0.00	0.00
Sb	0.00	1.21	27.70	25.86	23.80	0.00	23.29	5.68	30.29	5.65
Pb	0.00	0.23	0.00	0.00	0.25	0.00	0.00	0.00	0.19	0.19
Bi	0.00	0.14	0.00	0.00	0.08	0.00	0.00	0.00	0.07	0.17
As	18.47	19.53	2.64	3.47	3.50	22.17	4.90	16.08	1.00	15.65
Te	0.00	0.00	0.00	0.00	2.30	0.00	0.00	0.00	0.00	0.00
S	28.20	28.49	24.74	25.32	24.61	27.99	26.42	27.72	25.21	27.94
Total	99.38	100.95	101.28	100.86	99.81	100.63	101.25	100.52	101.65	100.91
Structural formula										
Mn	0.000	0.006	0.000	0.005	0.000	0.000	0.000	0.000	0.003	0.000
Fe	1.082	0.946	0.661	0.174	0.206	0.501	0.182	0.183	0.295	1.845
Co	0.000	0.003	0.003	0.000	0.000	0.000	0.006	0.000	0.000	0.007
Ni	0.000	0.004	0.000	0.000	0.000	0.000	0.000	0.000	0.000	0.003
Cu	9.976	9.786	9.188	9.155	9.840	9.734	9.637	9.893	9.079	10.314
Zn	1.265	1.082	1.322	1.737	1.520	1.590	1.928	1.935	1.459	0.023
Au	0.000	0.015	0.001	0.003	0.008	0.000	0.000	0.000	0.016	0.011
Ag	0.016	0.017	0.652	0.498	0.262	0.006	0.125	0.018	0.437	0.020
Cd	0.000	0.008	0.002	0.007	0.004	0.002	0.005	0.000	0.049	0.003
In	0.000	0.004	0.000	0.000	0.000	0.000	0.000	0.000	0.000	0.000
Sb	0.000	0.145	3.833	3.496	3.309	0.000	3.117	0.701	4.127	0.693
Pb	0.000	0.016	0.000	0.000	0.020	0.000	0.000	0.000	0.015	0.013
Bi	0.000	0.010	0.000	0.000	0.007	0.000	0.000	0.000	0.006	0.012
As	3.643	3.777	0.593	0.762	0.791	4.405	1.065	3.227	0.222	3.116
Te	0.000	0.000	0.000	0.000	0.306	0.000	0.000	0.000	0.000	0.000
S	13.000	13.000	13.000	13.000	13.000	13.000	13.000	13.000	13.000	13.000
Total	28.982	28.819	29.255	28.837	29.273	29.238	29.065	28.957	28.708	29.060

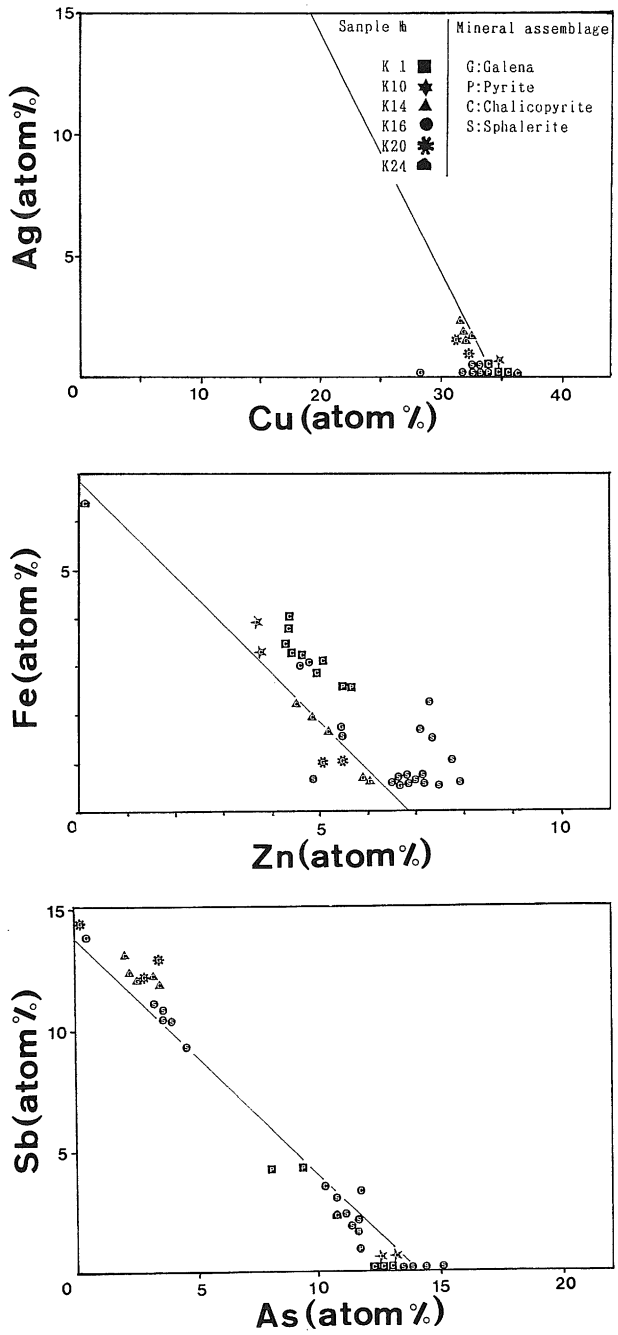

Fig. 12. Cu–Ag, Fe–Zn and As–Sb variations of tetrahedrite and tennantite. Straigft lines represent ideal substitutions by $Cu \rightleftarrows Ag$, $Fe \rightleftarrows Zn$ and $As \rightleftarrows Sb$, when the chemical formula is assumed to be $(Cu, Ag)_{10}(Fe, Zn)_2(Sb, As)_4S_{13}$.

occurs in chalcopyrite and sphalerite, as unhedral grains, less than 0.05 mm in diameter, and as veinlet.

As indicated in Table 6 and Fig. 12, compositional variations by substitutions of Sb ⇋ As, Ag ⇋ Cu and Fe ⇋ Zn are remarkable. Generally tetrahedrite and tennantite are rich in Zn. Tetrahedrite associated with pyrite and chalcopyrite tends to

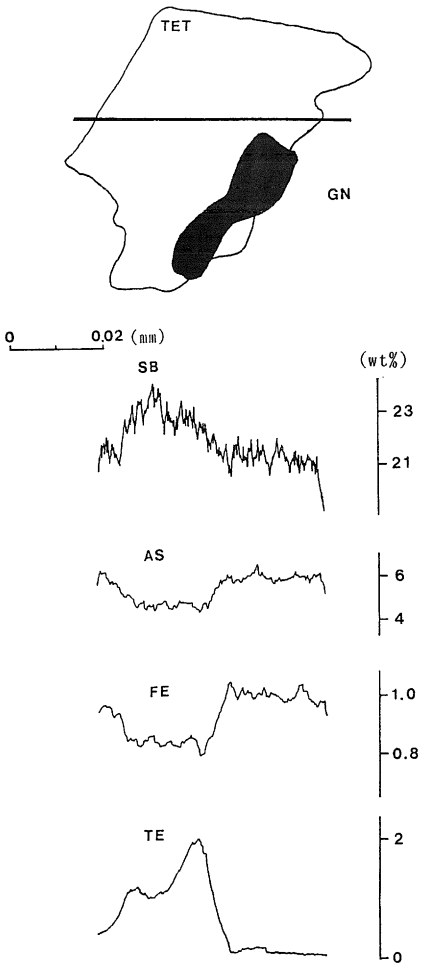

Fig. 13. Line scan profile of tetrahedrite. Horizontal line in tetrahedrite is position of line scan. TET: tetrahedrite, GN: galena.

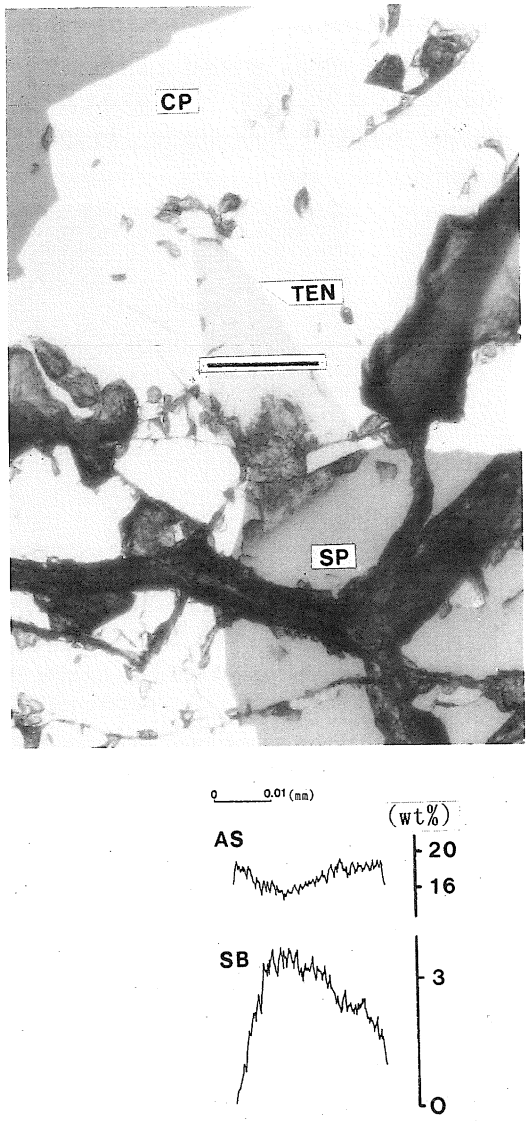

Fig. 14. Line scan profile of tennantite. Horizontal line in tennantite is scanning position. TEN: tennantite, CP: chalcopyrite, SP: sphalerite.

contain more Fe than that with sphalerite and galena. A part of thtrahedrite contains moderate amount of Ag (Nos. K14-501, -502, -506 and -507). Even in the one grain, the tetrahedrite and tennantite are very heterogeneous in composition (Figs. 13 and 14). As indicated in Fig. 13, there are Te-rich regions in the tetrahedrite grain, whose Te content attains to 2.30 wt.% (No. K14-507 in Table 6).

Luzonite and enargite

Luzonite occurs around euhedral to subhedral pyrite crystals in chalcopyrite (MUKAIYAMA et al., 1974). It also occurs as veinlet in pyrite, sphalerite and chalcopyrite, and as dots in chalcopyrite. In sphalerite, luzonite fills the cavities with pyrite,

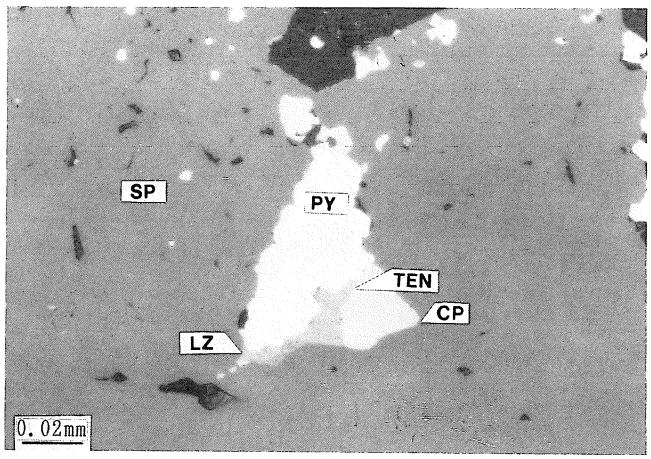

Fig. 15. Photomicrograph showing luzonite (LZ), pyrite (PY), tennantite (TEN) and chalcopyrite (CP) in sphalerite (SP).

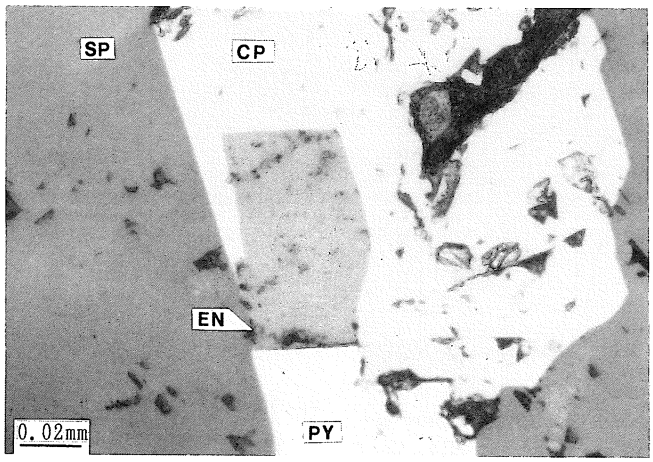

Fig. 16. Euhedral enargite (EN) in chalcopyrite (CP).

tennantite and chalcopyrite (Fig. 15). The reflection color is pinkish grey. The reflection pleochroism and anisotropy under crossed nicols are distinct, and lamellar twinning is observed.

Enargite occurs as euhedral crystal, about 0.08 mm in length, with pyrite and chalcopyrite in sphalerite grain (Fig. 16). The reflection color is blueish green, and the reflection pleochroism is weak.

As listed in Table 7, luzonite and enargite contain 1–3 wt.% of Fe and 0–2 wt.% of Zn.

Bornite

The dots of bornite, less than 0.01 mm in diameter, occur with covellite, chalcopyrite and galena in pyrite grain (Fig. 7).

Table 7. EPMA analyses of luzonite-enargite

	K10-601	K20-602	K24-601	K24-602
Fe	1.46	2.06	3.29	1.01
Co	0.01	0.01	0.01	0.00
Ni	0.00	0.00	0.00	0.02
Cu	46.48	47.22	46.00	48.82
Zn	1.61	0.05	0.37	0.16
Au	0.03	0.05	0.04	0.06
Ag	0.02	0.02	0.06	0.02
Cd	0.00	0.00	0.02	0.00
Pb	0.14	0.19	0.05	0.08
Bi	0.24	0.29	0.21	0.23
As	17.29	18.36	17.38	18.00
S	33.10	31.76	32.80	31.10
Total	100.38	100.01	100.23	99.50
Structural formula				
Fe	0.101	0.149	0.230	0.074
Co	0.001	0.000	0.000	0.000
Ni	0.000	0.000	0.000	0.001
Cu	2.834	3.000	2.830	3.168
Zn	0.095	0.003	0.022	0.010
Au	0.001	0.001	0.001	0.001
Ag	0.001	0.001	0.002	0.000
Cd	0.000	0.000	0.001	0.000
Pb	0.003	0.004	0.001	0.002
Bi	0.004	0.006	0.004	0.005
As	0.894	0.989	0.907	0.991
S	4.000	4.000	4.000	4.000
Total	7.934	8.153	7.998	8.252

Table 8. EPMA analyses of bornite

	K14-701	K16-701	K16-702	K24-701
Mn	0.00	0.02	0.02	0.00
Fe	13.21	14.17	14.16	11.53
Co	0.02	0.05	0.05	0.03
Ni	0.00	0.04	0.11	0.01
Cu	59.94	56.10	55.52	61.37
Zn	0.02	0.15	0.12	0.03
Au	0.18	0.33	0.24	0.00
Ag	0.56	1.32	1.63	0.00
Cd	0.00	0.04	0.04	0.02
In	0.00	0.05	0.01	0.00
Pb	0.50	0.07	0.20	0.11
Bi	0.15	0.16	0.19	0.14
As	0.07	0.01	0.08	0.00
S	25.12	27.33	29.12	26.25
Total	99.77	99.84	101.49	99.49
Structural formula				
Mn	0.000	0.001	0.002	0.000
Fe	1.204	0.893	1.116	1.008
Co	0.002	0.003	0.004	0.002
Ni	0.002	0.002	0.008	0.002
Cu	4.799	3.107	3.847	4.718
Zn	0.002	0.008	0.008	0.002
Au	0.005	0.006	0.005	0.000
Ag	0.027	0.043	0.066	0.000
Cd	0.027	0.001	0.002	0.000
In	0.000	0.002	0.000	0.000
Pb	0.012	0.001	0.004	0.003
Bi	0.004	0.003	0.004	0.003
As	0.005	0.001	0.005	0.000
S	4.000	3.000	4.000	4.000
Total	10.089	7.071	9.071	9.738

Representative analyses are listed in Table 8. Although chemical formula is similar to ideal Cu_5FeS_4, Cu and Fe contents vary by the Cu $\leftrightharpoons$ Fe substitution. It is interesting that the chemical formula of No. K16-701 and K16-704, which coexist with covellite, should be represented to be Cu_3FeS_3 and Cu_4FeS_4, respectively, although minerals of these chemical formula have not been reported.

Covellite

Covellite occurs as dots, about 0.01 mm in diameter, with bornite and chalcopyrite

Table 9. EPMA analyses of covellite

	K10-801	K20-801
Fe	0.03	0.66
Co	0.00	0.03
Ni	0.01	0.04
Cu	58.64	62.00
Zn	1.64	0.66
Au	0.00	0.35
Ag	6.70	0.00
Cd	0.00	0.10
Pb	2.74	0.00
Bi	0.16	0.00
As	0.00	0.66
S	29.60	34.69
Total	99.52	99.19
Structural formula		
Fe	0.001	0.000
Co	0.000	0.000
Ni	0.000	0.001
Cu	0.999	0.902
Zn	0.027	0.002
Au	0.000	0.002
Ag	0.067	0.000
Cd	0.000	0.001
Pb	0.014	0.000
Bi	0.001	0.000
As	0.000	0.008
S	1.000	1.000
Total	2.109	1.916

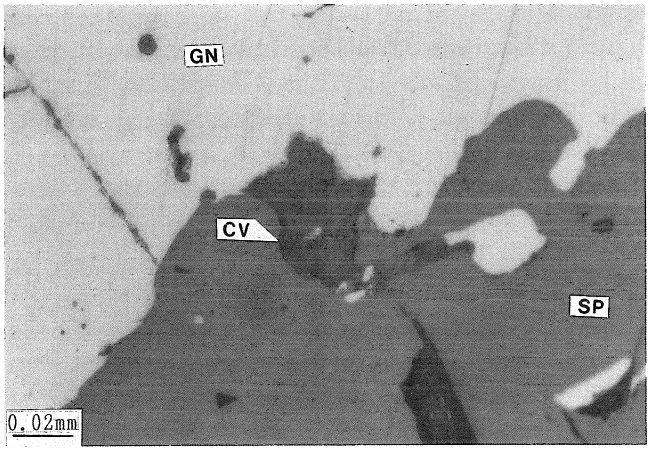

Fig. 17. Ag-rich covellite (CV) in sphalerite (SP).

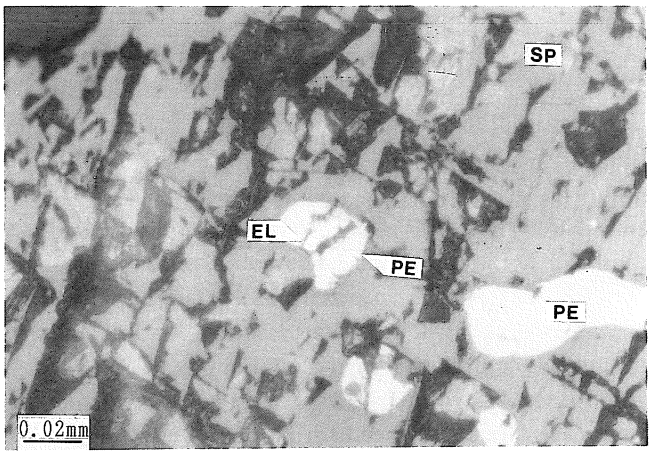

Fig. 18. Electrum (EL) and petzite (PE) in sphalerite (SP).

in pyrite grain (Fig. 7), and as veinlets in the fractures or cleavages in the sphalerite, galena, pyrite and chalcopyrite.

A part of covellite (Fig. 17) contains Ag up to about 7 wt.% (No. K10-801 in Table 9).

Electrum and Au-Ag-Te minerals

Rarely, very fine electrum grain, 0.03 mm in diameter, occurs with Au-Ag-Te minerals in sphalerite (Fig. 18). The Au-Ag-Te minerals occur in sphalerite and galena, and are sylvanite ($AuAgTe_4$), petzite (Ag_3AuTe_2) and hessite (Ag_2Te), which are about 0.1 mm in diameter (Fig. 19).

The chemical compositions are listed in Table 10. The electrum and Au-Ag-Te

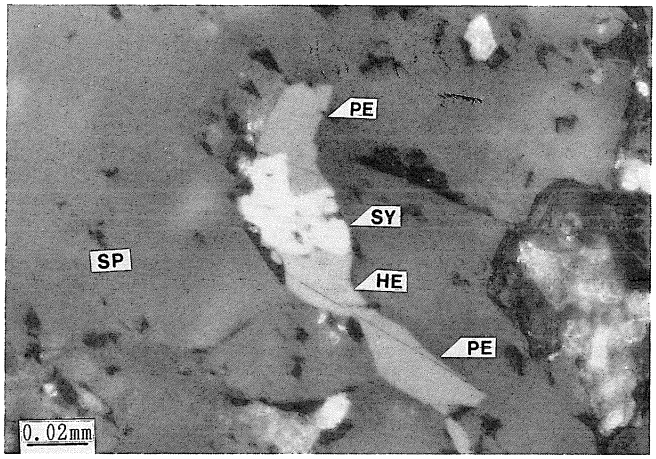

Fig. 19. Petzite (PE), sylvanite (SY) and hessite (HE) in shpalerite (SP).

Table 10. EPMA analyses of Au-Ag-Te series mineral and electrum

	K20-902	K20-903	K20-905	K20-906	K20-907
Fe	0.00	0.00	0.00	0.00	0.15
Co	0.00	0.00	0.00	0.00	0.02
Cu	0.06	0.03	0.03	0.00	0.07
Zn	2.53	0.89	2.27	1.18	2.15
Au	0.29	0.23	21.15	24.07	86.75
Ag	62.26	62.91	43.00	12.94	10.01
Cd	0.14	0.12	0.06	0.00	0.00
Bi	0.05	0.08	0.18	0.00	0.30
Te	35.63	35.73	31.70	62.65	0.13
Total	100.96	99.99	98.39	100.84	99.58
Structural formula					
Fe	0.000	0.000	0.000	0.000	0.005
Co	0.000	0.000	0.000	0.000	0.001
Cu	0.003	0.002	0.004	0.000	0.002
Zn	0.139	0.048	0.279	0.148	0.058
Au	0.005	0.004	0.865	0.995	0.768
Ag	2.067	2.083	3.209	0.997	0.162
Cd	0.004	0.004	0.004	0.000	0.000
Bi	0.001	0.001	0.007	0.000	0.002
Te	1.000	1.000	2.000	4.000	0.002
Total	3.219	3.142	6.368	6.140	1.000

minerals contain small amount of Zn.

Gangue minerals

Quartz is the most dominant gangue mineral. It fills the fractures in the sulfide minerals, and forms euhedral crystals in the cavities. It includes fine grained sulfide minerals. Chlorite and illite occur in the cavities of ores. Calcite and small amount of siderite occur as small grains or veinlets in the high-grade ores.

Discussion

Ore minerals and mineral compositions

Although the Iwami kuroko deposits were one of the typical kuroko type deposits in Japan, ore minerals reported so far are only sphalerite, galena, pyrite, chalcopyrite, tetrahedrite, luzonite (MUKAIYAMA et al., 1974) and bornite (URABE, 1974a). In addition to these minerals, we confirmed tennantite, enargite, covellite, electrum, sylvanite, petzite and hessite. Most of these minerals have been confirmed in other kuroko mines, which is summarized in SHIMAZAKI (1974) and MATSUKUMA (1989). Whereas Au-Ag-Te minerals, such as sylvanite, petzite and hessite, have been not reported. MATSUKUMA (1989) mentioned that tellurides have not been found from any kuroko deposits. However, as indicated clearly in the present study, Au-Ag-Te minerals are ore minerals of kuroko deposit.

Chemical compositions of sphalerite from the Iwami mine have been reported by MUKAIYAMA et al (1974) and URABE (1974a). The present results are consistent with theirs. YUI (1984) suggested that the yellow brown-reddish brown part in sphalerite is due to relatively high Cu, As and Sb contents. In the present study, it was found that the reddish brown band in sphalerite is relatively high in Cu content, whereas As and Sb variations are not observed.

The chemical compositions of other ore minerals from the Iwami kuroko deposits have been not reported. The present results of chemical analyses for ore minerals show that the minerals are generally variable in composition, as described before. It is interesting that in pyrite there is a part where Cu and As contents attain to 1.79 and 0.85 wt.%, respectively, that dots of chalcopyrite in pyrite contain Ag up to 1.49 wt.%, and that a part of covellite contains moderate amount of Ag. In this paper, the minerals whose chemical formulae are Cu_3FeS_3 and Cu_4FeS_4 are described as bornite. However further investigation is needed.

The tetrahedrite-tennantite minerals in the present study are generally rich in Zn. SHIKAZONO and KOUDA (1979) suggested that, in Zn-rich tetrahedrite, Cu+Ag and Zn+Fe values deviate from the ideal chemical formula, $(Cu, Ag)_{10}(Zn, Fe)_2 (As, Sb)_4S_{13}$, and that the chemical forumula should be represented to be $(Cu, Ag, Zn, Fe)_{12}(As, Sb)_4S_{13}$. In fact, as indicated in Fig. 12, Cu+Ag values are generally less and Fe+Zn

values are more than the ideal values of the formula, $(Cu, Ag)_{10}(Zn, Fe)_2 (As, Sb)_4S_{13}$, suggesting that moderate amount of Fe+Zn occupies (Cu, Ag)-site. YAMAOKA and NEDACHI (1980) also reported the same tendency for tetrahedrite from kuroko deposits. Since this phenomenon is observed in Zn-rich teterahedrite, it is speculated that moderate amount of Zn occupies (Cu, Ag)-site (SHIKAZONO and KOUDA, 1979). Although tetrahedrite-tennantite mineral in the Iwami deposits shows considerable variation in As and Sb, As-rich species are more than Sb-rich ones. This is consistent with the suggestion by SHIKAZONO and KOUDA (1979). The zonal structure of tetrahedrite-tennantite series minerals has been studied by YAMAOKA (1969), YUI (1971), SHIMAZAKI (1974), YAMAOKA and NEDACHI (1980), HACKBARTH and PETERSEN (1984) and SHIMA (1988). The tetrahedrite-tennantite minerals in the present study also show zonal structure by Sb ⇋As substitution. Generally Fe and Te show more complex variations than those shown in Fig. 13.

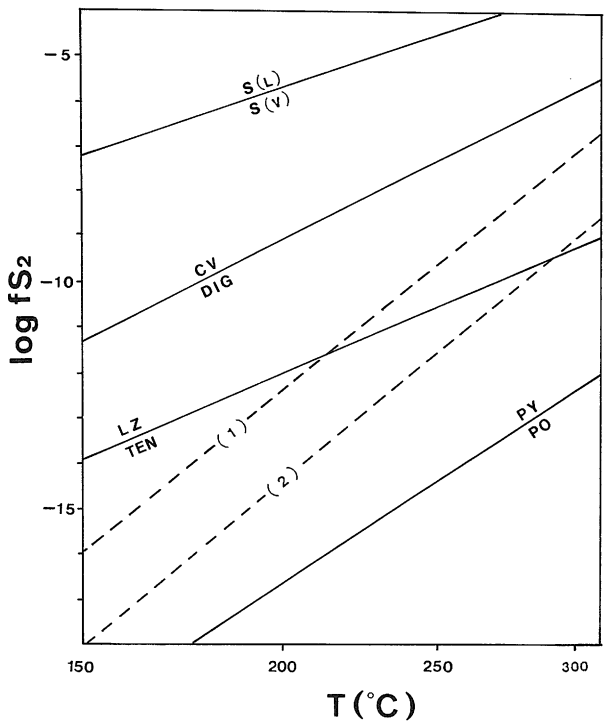

Fig. 20. Log fS_2-temperature diagram for common sulfides and sulfosalts (after BARTON and SKINNER, 1966; URABE, 1974b).
PO: pyrrhotite, PY: pyrite, DIG: digenite, CV: covellite, LZ: luzonite, TEN: tennantite, S(V): sulfur vapor, S(L): sulfur liquid, (1): 0.1 mol% FeS of sphalerite, (2): 1.0 mol% FeS of sphalerite.

Mineralization sequence and conditions

By the petrographical observations on the textures of ore minerals, mineralization sequence of the network and disseminated deposits may be speculated as follows; first, a large amount of quartz crystallized with fine grained pyrite. Second, sphalerite and galena crystallized mainly with small amounts of chalcopyrite and tetrahedrite. Electrum and Au-Ag-Te minerals (sylvanite, petzite and hessite) are regarded to have crystallized in this stage, because these occur only in sphalerite and galena. Next, coarse grained pyrite, associated with small amounts of bornite and covellite, and chalcopyrite, associated with tennantite, luzonite and calcite, crystallized. Finally, small amounts of luzonite, covellite, calcite and siderite formed veinlets in ore minerals previously crystallized.

MUKAIYAMA et al. (1974) estimated the temperature of ore formation by the data of filling temperatures of inclusions in sphalerite and quartz; higher temperatures of the netwrok deposits are 200–250°C, which are consistent with those of bedded kuroko deposits, and the lowest temperatures 177–192°C. By using FeS content in the sphalerite, YOSHIDA et al. (1977) estimated fS_2 to be 10^{-13}–$10^{-9.5}$ atm. If this fS_2 condition is assumed to have been almost constant during the mineralization, crystallization of luzonite and covellite in the last stage can be well explained by the decreasing temperature (Fig. 20).

Acknowledgments

We are grateful to Mr. I. AMANO of the Iwami Mine Co., Ltd. for his help on collecting samples. We thank to Prof. H. SHIMA and Associate Prof. T. MIZOTA for their kindly giving us some synthetic sulfide minerals as EPMA standards. We also thank to Profs. I. SHIMADA, S. IIZUMI, Associate Profs. Y. SAWADA, Y. MIYAKE, K. TAZAKI and A. TAKASU for their valuable and constructive advices.

References

BARTON, P. B., Jr. and TOULMIN, P., III., 1966: Phase relations involving sphalerite in the Fe-Zn-S system. *Econ. Geol.*, **61**, 815–849.

HACKBARTH, C. and PETERSEN, U., 1984: A fractional crystallization model for the deposition of argentian tetrahedrite. *Econ. Geol.*, **79**, 448–460.

IKEDA, A., 1985: Iwami mine, *in* Geology of Shimane, 448–450, Shimane Prefecture, Shimane**.

MATSUKUMA, T., 1989: Ore microscopy of the kuroko ores in Japan. Toko Printing Co. Ltd., Sendai.

MITI, 1967: Report on the regional geological survey, Shimane district of the 1966's fiscal year. Ministry Intern. Trade Indus., 1–26*.

MUKAIYAMA, H., MONONOBE, S. and YOSHIDA, T., 1974: Genesis of the ore deposits of the Iwami mine, Shimane Prefecture, Japan. *Mining Geol., Special Issue,* **6**, 221–234.

SHIKAZONO, N. and KOUDA, R., 1979: Chemical composition of tetrahedrite-tennantite minerals and the chemical environments of some Japanese ore deposits. *Mining Geol.*, **29**, 33–41*.

SHIMA, H., 1988: Growth texture of ore minerals.*In* SUGAKI, A. (ed.), Ore microscope and ore texture, 133–146, TERRA SCI. PUB. COM., Tokyo**.

SHIMAZAKI, Y., 1974: Ore minerals of the kuroko-type deposits. *Mining Geol., Special Issue,* **6**, 311–322.

URABE, T., 1974a: Iron content of sphalerite coexisting with pyrite from some kuroko deposits. *Mining Geol., Special Issue,* **6**, 377–384.

URABE, T., 1974b: Mineralogical aspect of kuroko deposits in Japan and their implications. *Mineral. Deposita (Berl.)*, **9**, 309–324.

YAMAOKA, K., 1969: On ore minerals from the kuroko deposits in the Tohoku district. *In* Symposium: Crystallograpy and geochemistry on minerals from kuroko deposits and sulfide minerals from hydrothermal deposits, 1–37**.

YAMAOKA, K. and NEDACHI, M., 1980: Minerals of the tetrahedrite-tennantite series from the Kuroko deposits and their zonal structure. *J. Japan. Assoc. Min. Pet. Econ. Geol., Spec. Issue,* **2**, 97–104*.

YOSHIDA, T., IZAWA, E. and MORIMOTO, N., 1977: The hydrothermal alteration in the kuroko-type stockwork deposits at the Iwami mine, Shimane Prefecture, Japan. *Mining Geol.,* **27**, 181–189*.

YUI, S., 1971: Heterogeneity within a single grains of minerals of tennantite-tetrahedrite series. *Mining Geol., Spec. Issue,* **2**, 22–29.

* In Japanese with English abstract

** In Japanese